SUPPLEMENTAL DATA

1. **Supplemental Figure 1-Supplemental Figure 22**
2. **Supporting Table 1 and Supporting Table 2**

HMGB1 Promotes Ductular Reaction and Tumorigenesis in Autophagy-deficient Livers

Bilon Khambu, Nazmul Huda, Xiaoyun Chen, Yong Li, Guoli Dai, Ulrike A. Köhler, Wei-Xing Zong, Satoshi Waguri, Sabine Werner, Tim D. Oury, Zheng Dong, Xiao-Ming Yin

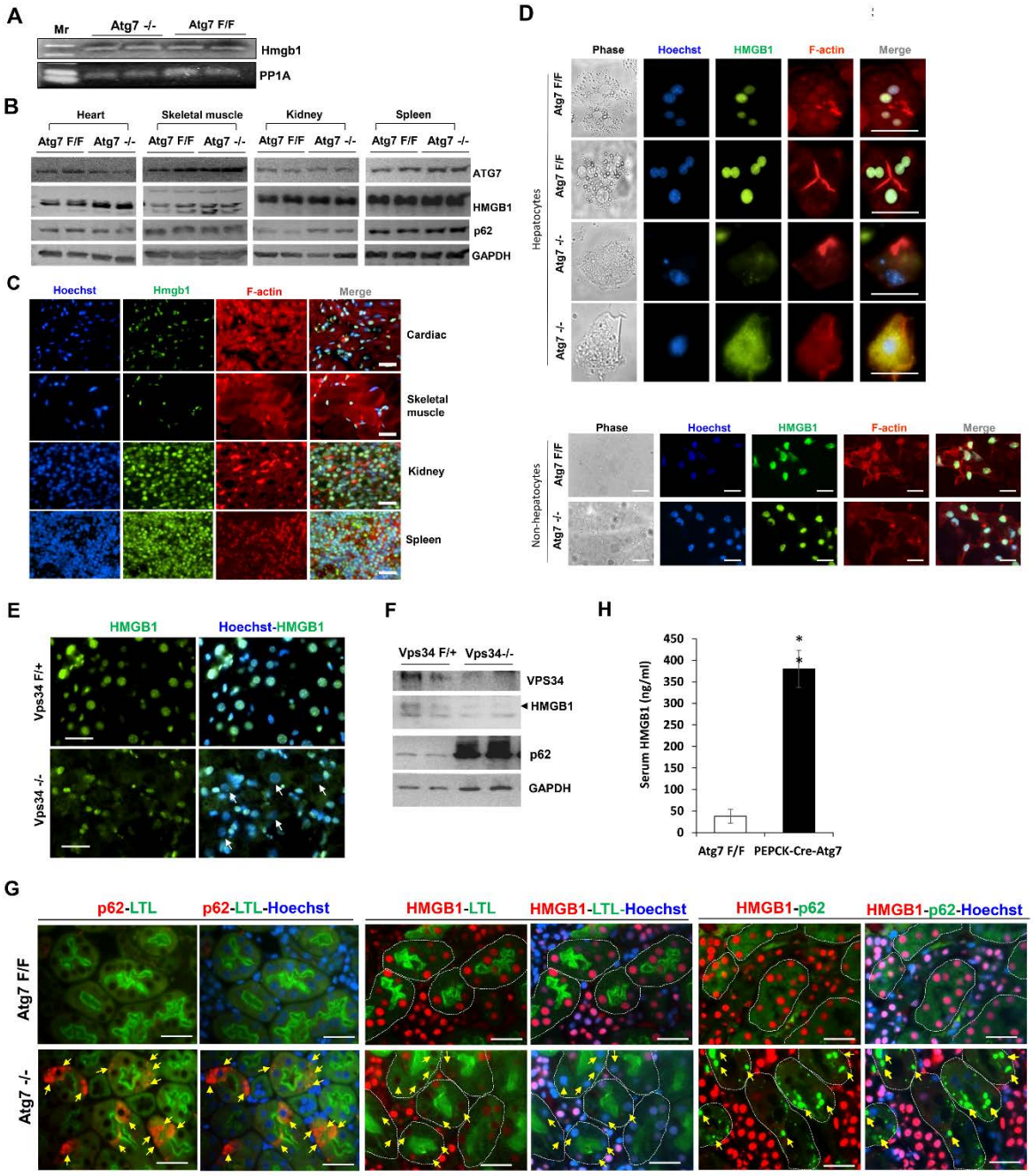

Supplemental Figure 1. HMGB1 release is specific to autophagy-deficiency. (**A**) Hepatic mRNA levels of HMGB1 in *Atg7* F/F and *Atg7*$^{\Delta Hep}$ (*Atg7-/-*) mice were determined by RT-PCR. Mr. = molecular weight. (**B-C**) Liver lysates or liver sections from *Atg7* F/F and *Atg7*$^{\Delta Hep}$ mice were examined by immunoblotting (B) or immunostaining (C) assay. (**D**) Primary hepatocytes and non-parenchymal cells were separated from collagenase-perfused livers of *Atg7* F/F and *Atg7*$^{\Delta Hep}$ mice, and stained for HMGB1. (**E-F**) Liver sections or lysates from 9-week old *Vps34*

F/+ and *Vps34*$^{\Delta Hep}$ (*VPS34-/-*) mice were subjected to immunostaining (E) or immunoblotting (F) assay. Arrows indicate hepatocytes without nuclear HMGB1 staining (E). Each lane represents one sample (F). (**G**) Three groups of double staining of the kidney sections of the Atg7 F/F and PEPCK-Cre-Atg7 (*Atg7-/-*) mice. Proximal tubules in which Atg7 is deleted in the PEPCK-Cre-Atg7 mice are indicated by the positive staining of FITC-Lotus Tetragonolobus Lectin (LTL). Some tubules are traced with dotted lines for recognition. Increased p62 expression and aggregation was detected in many cells of the proximal tubules in the kidney of the PEPCK-Cre-Atg7 mice, in which nuclear HMGB1 was largely undetected. Arrows indicate p62 aggregates (red) in p62-LTL double staining, HMGB1 (red)-depleted nuclei in HMGB1-LTL double staining, and p62 aggregates (green) in HMGB1-p62 double staining. (**H**) Increased HMGB1 was detected in the serum of PEPCK-Cre-Atg7 mice. Data shown are mean ± SEM. *: $p<0.05$, two-side *Student's* t test (n = 3 mice/group). Scale bar: 10 μm.

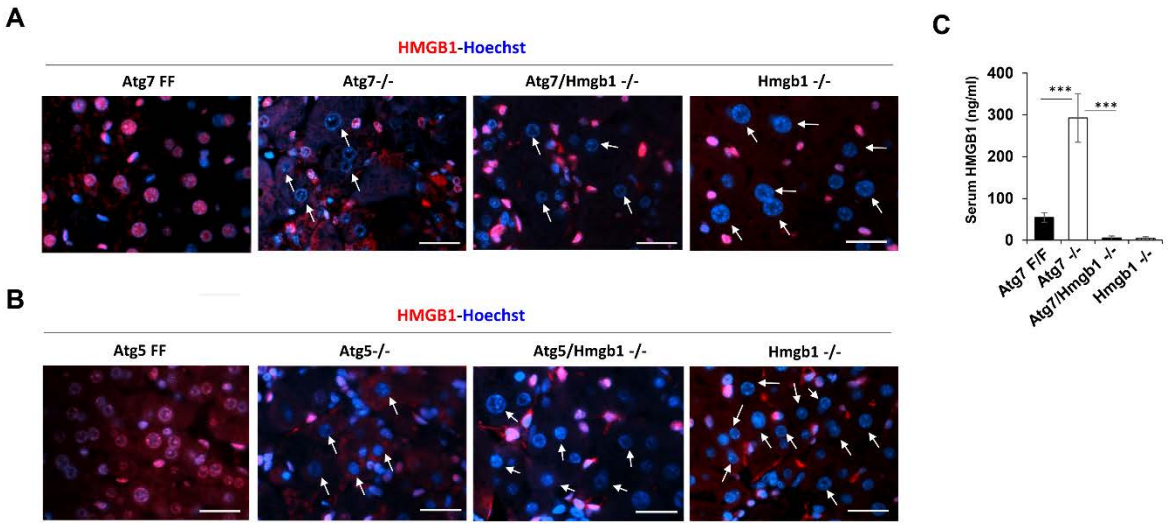

Supplemental Figure 2. Lack of HMGB1 in *Hmgb1*$^{\Delta Hep}$ hepatocytes. (A-B) Liver sections from *Atg7*$^{\Delta Hep}$ (*Atg7-/-*) (A) or *Atg5*$^{\Delta Hep}$ (*Atg5-/-*) (B) mice with or without *Hmgb1*$^{\Delta Hep}$ were immunostained with anti-HMGB1 antibody. Arrows indicate hepatocytes in which HMGB1 staining (red) was absent. (**C**) Serum levels of HMGB1 were determined by ELISA (n=3 mice per group). Data shown are mean ± SEM. ***: $p<0.001$, one-way ANOVA with Duncan's methods post-hoc analysis. Scale bar: 10 µm.

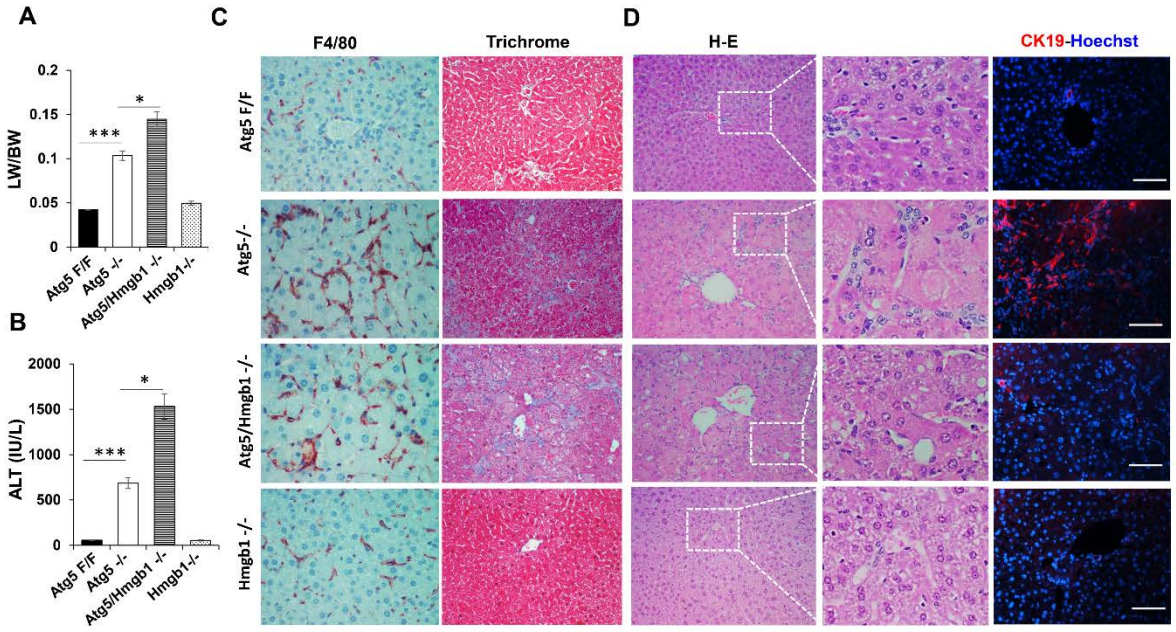

Supplemental Figure 3. Hepatic HMGB1 does not promote inflammation or fibrosis in *Atg7*-deficient livers. (**A**) Liver lysates from 9-week old mice of different genotypes were analyzed by immunoblotting assay. (**B**) Liver sections from mice of different genotypes were stained for F4/80, MPO, CD3 or CD45R (400x). Quantification of F4/80-positive cells was shown in Figure 2E. (**C**). Liver sections from mice of different genotypes were stained with Trichrome (400x) or with Sirius Red (200x) or anti-Desmin. Quantification of the fibrotic area based on Trichrome staining was shown in Figure 2F. (**D-E**) Hepatic mRNA levels of *Col1a1* and *Ctgf* were determined by qRT-PCR (n=3 mice/group). (**F**) The level of α-hydroxyproline was measured and normalized to the weight (mg) of liver tissue analyzed (n= 3 mice/group). Data shown are mean ± SEM. *: $p<0.05$; ***: $p<0.001$, n.s.: no significance; by one-way ANOVA with Duncan's methods post-hoc analysis. Scale bar: 50 μm.

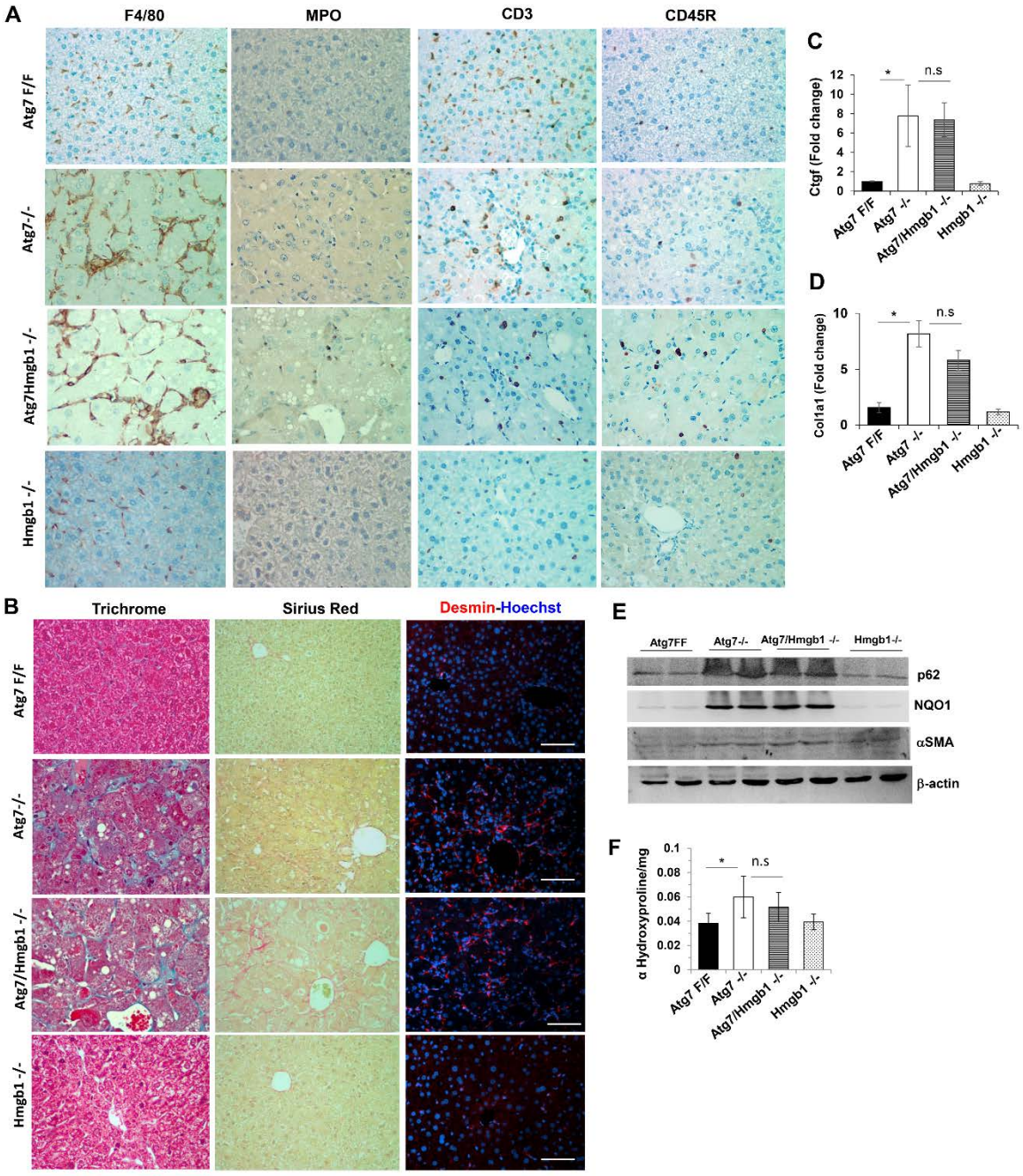

Supplemental Figure 4. Hepatic HMGB1 does not promote injury, inflammation or fibrosis, but promotes DR in *Atg5*-deficient livers. (**A-B**) Samples from 9-week old *Atg5* F/F (n= 4), *Atg5*$^{\Delta Hep}$ (*Atg5*-/-) (n= 4), *Atg5*$^{\Delta Hep}$/*Hmgb1*$^{\Delta Hep}$ *(Atg5/Hmgb1 -/-)* (n=5) and *Hmgb1 -/-* (n=6) mice were analyzed for liver weight (LW)/body weight (BW) ratio (A), and serum levels of ALT (B). (**C-D**) Liver sections from mice of different genotypes were stained for F4/80 or Trichrome-stained (C), or were H-E stained or stained for CK-19 (D). Images for histology were

taken at 200x magnification. Data shown are mean ± SEM. *: $p<0.05$, ***: $p<0.001$; by one-way ANOVA with Duncan's methods post-hoc analysis. Scale bar: 50 μm.

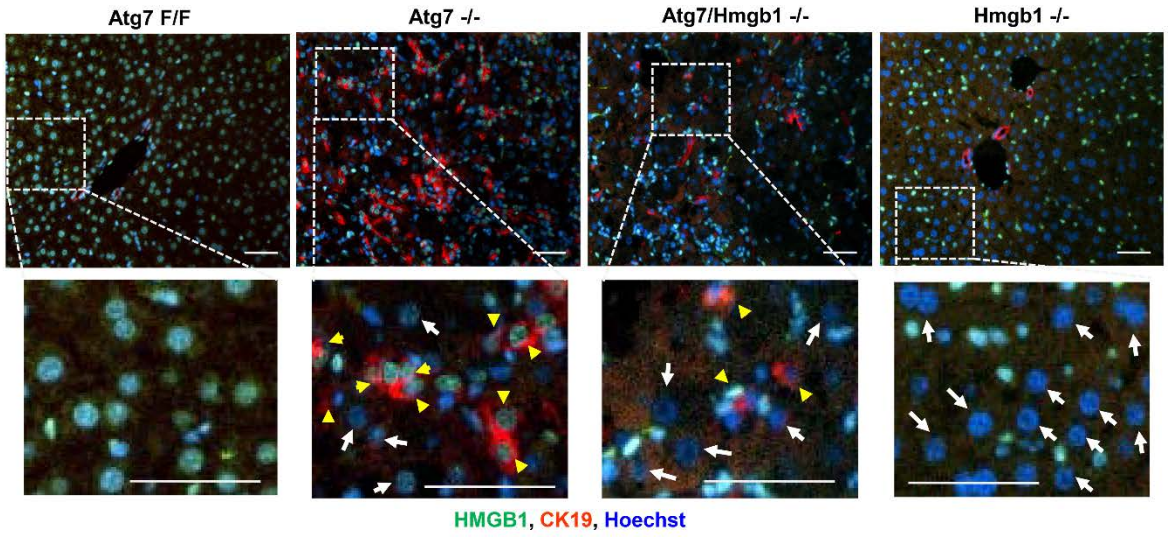

Supplemental Figure 5. HMGB1 remains required for the expansion of ductular cells in aged autophagy deficient livers. Livers from 9-month old mice of different genotypes were immunostained with anti-HMGB1 antibody (green) and anti-CK19 (red), and counter-stained with Hoechst 33342 (blue) for the nucleus. Framed areas in the upper row are enlarged in the lower row. White arrows indicate nuclei of hepatocytes, which lacked HMGB1 staining. Yellow arrowheads indicate CK19-positive ductular cells, which were positive for HMGB1. Scale bar: 50 μm.

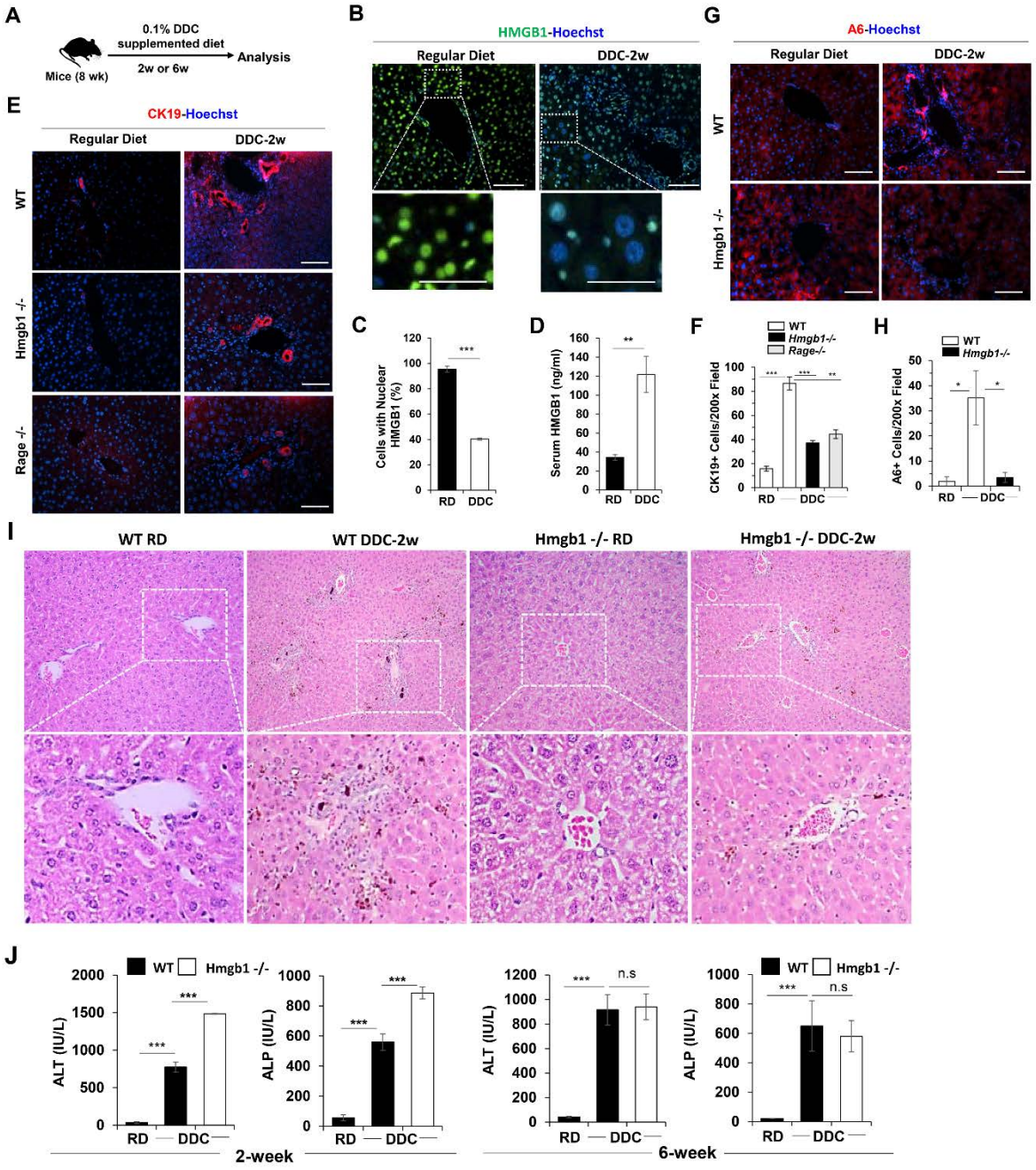

Supplemental Figure 6. *Hmgb1*$^{\Delta Hep}$ mice exhibit reduced ductular reaction in response to DDC diet. (**A**) Scheme of the DDC diet regime. (**B**) Liver sections from wild type mice fed with control or DDC diet 2 week were stained for HMGB1. Framed areas were enlarged showing loss of hepatic nuclear HMGB1 in mice fed with DDC diet. (**C**) Quantification of cells with nuclear HMGB1. (**D**) Serum level of HMGB1 was measured by ELISA. (**E-H**) Liver sections from wild type, or *Hmgb1*$^{\Delta Hep}$ *(Hmgb1-/-), or Rage-/-* mice given the indicated diets for

2 weeks were immunostained for CK19 (E) or A6 (G), and positive cells were quantified (F, H). n=3 mice/group. (**I**) Liver sections from the mice fed with 2 weeks of DDC or regular diet were H-E stained (200x). (**J**) Serum levels of ALT and ALP in mice of different genotypes fed with regular or DDC diet for 2 or 6weeks. Data shown are mean ± SEM. *: $p<0.05$, ***: $p<0.001$; n.s.: no significance; by *Student's* t test (C, D) or one-way ANOVA with Duncan's post-hoc analysis (F, H, J). n=3-4 mice/group. Scale bar: 50 μm.

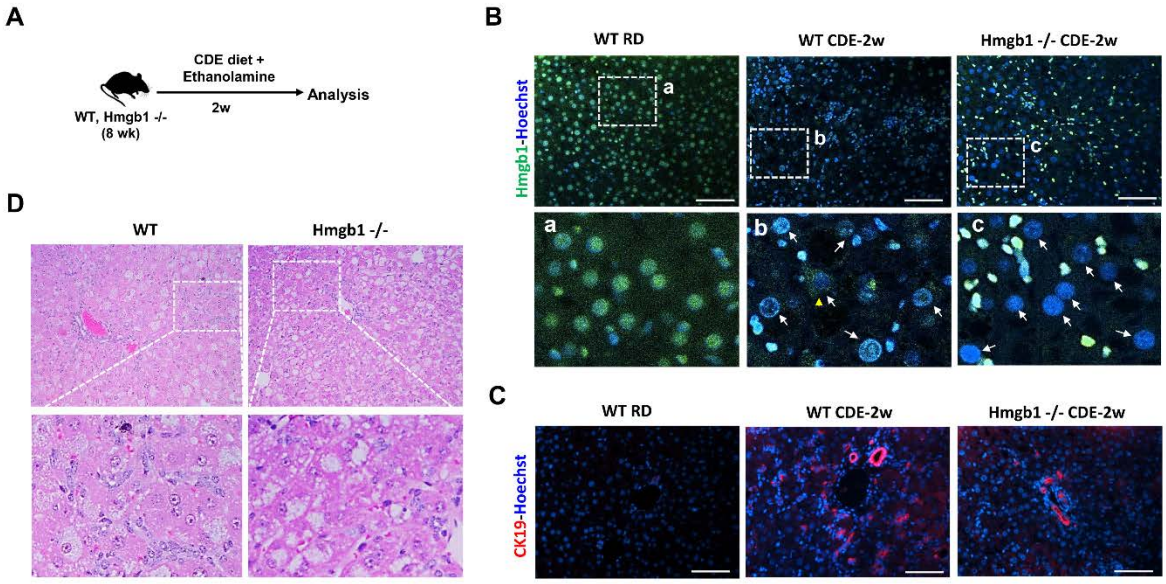

Supplemental Figure 7. *Hmgb1*$^{\Delta Hep}$ mice exhibit reduced ductular reaction in response to CDE diet. (**A**) Scheme of CDE diet regime. (**B-D**) Liver sections from wild type (WT) or *Hmgb1*$^{\Delta Hep}$ (*Hmgb1-/-)* mice given the indicated diets were immunostained for HMGB1 (B), or CK19 (C), or H-E stained (200x) (D). Framed areas (a-c) in B were enlarged in separate panels. The white arrows indicate hepatic nuclei that lost HMGB1, and the yellow arrowhead indicates the presence of cytosolic HMGB1 in one hepatocyte. Reduced ductular cell expansion was seen in *Hmgb1*$^{\Delta Hep}$ mice fed with CDE diet (C- D). Scale bar: 50 μm.

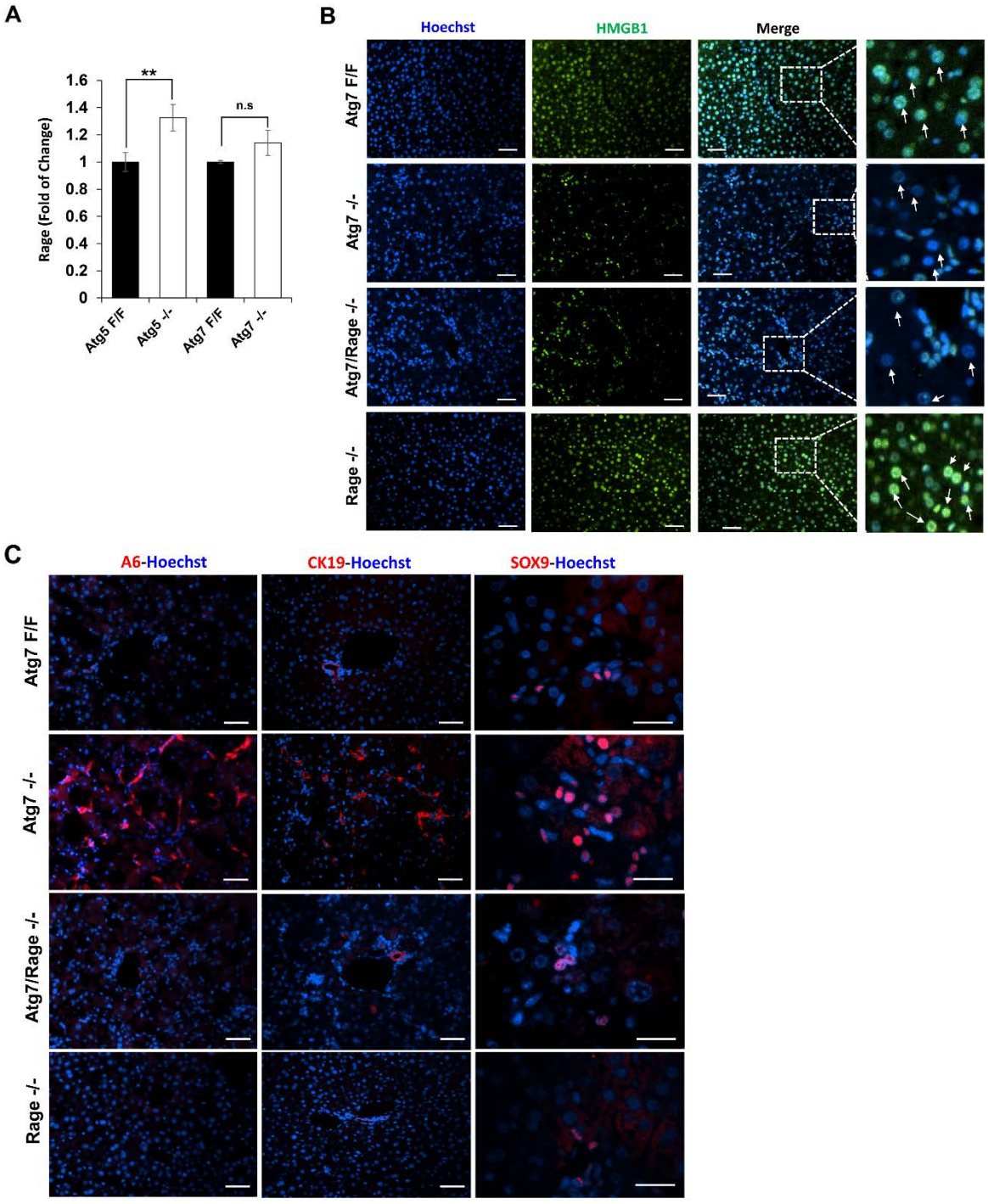

Supplemental Figure 8. RAGE is not required for HMGB1 release in autophagy deficient livers. (A) The mRNA level of RAGE in the liver was determined by qRT-PCR in the mice with designated genotypes (n=3 mice/group). (**B**) Liver sections of 9-week old mice with different genotypes were stained for HMGB1. Framed areas were enlarged and shown in

separate panels. Arrows indicate nuclei of hepatocytes, which were positive for HMGB1 in *Atg7 F/F* and *Rage* -/- liver, but negative for HMGB1 in *Atg7* -/- and *Atg7/Rage* -/- livers. (**C**). Liver sections of 9-week old mice with different genotypes were stained for CK19, A6, or SOX9. Quantification is presented in Figure 4E. Data shown are mean ± SEM. **: $p<0.01$; n.s.: no significance; by two-side *Student's* t-test. Scale bar: 50 μm. (panel B, A6, CK19 in panel C), 10 μm (SOX9 in panel C).

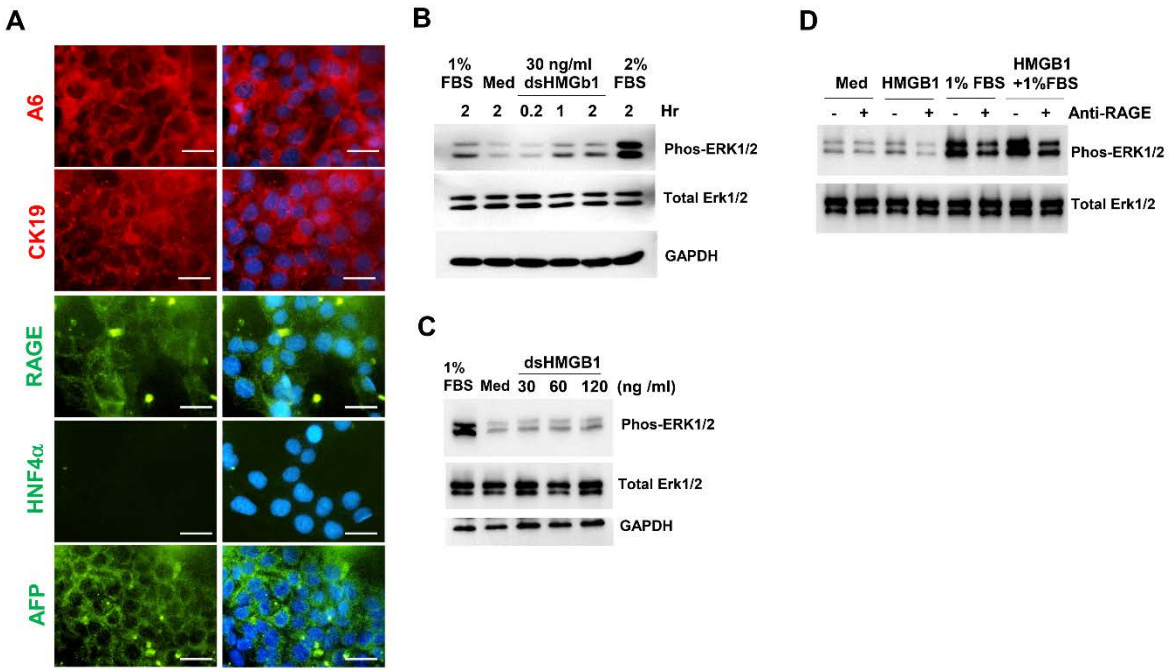

Supplemental Figure 9. BMOL cells express RAGE and respond to HMGB1 stimulation in a RAGE-dependent way. (**A**) BMOL cells were immunostained for the designated cellular markers. (**B)** BMOL cells were cultured in serum free medium (Med), or mediums supplemented with 1-2% FBS, or disulfide HMGB1 (dsHMGB1, 30 ng/ml) for 0.2 to 2 hours. Cell lysates were subjected to immunoblotting assay. (**C**) BMOL cells were cultured in serum free medium (Med), or Willman's E mediums supplemented with 1% FBS, or dsHMGB1 (30-120 ng/ml) for 2 hr. Cell lysates were subjected to immunoblotting assay. (**D**) BMOL cells were cultured in serum free medium (Med), or mediums supplemented with 1% FBS, and/or dsHMGB1 (60 ng/ml) in the presence or absence of an anti-RAGE antibody (2 µg/ml) for 2 hr. Cell lysates were subjected to immunoblotting assay. Scale bar: 10 µm.

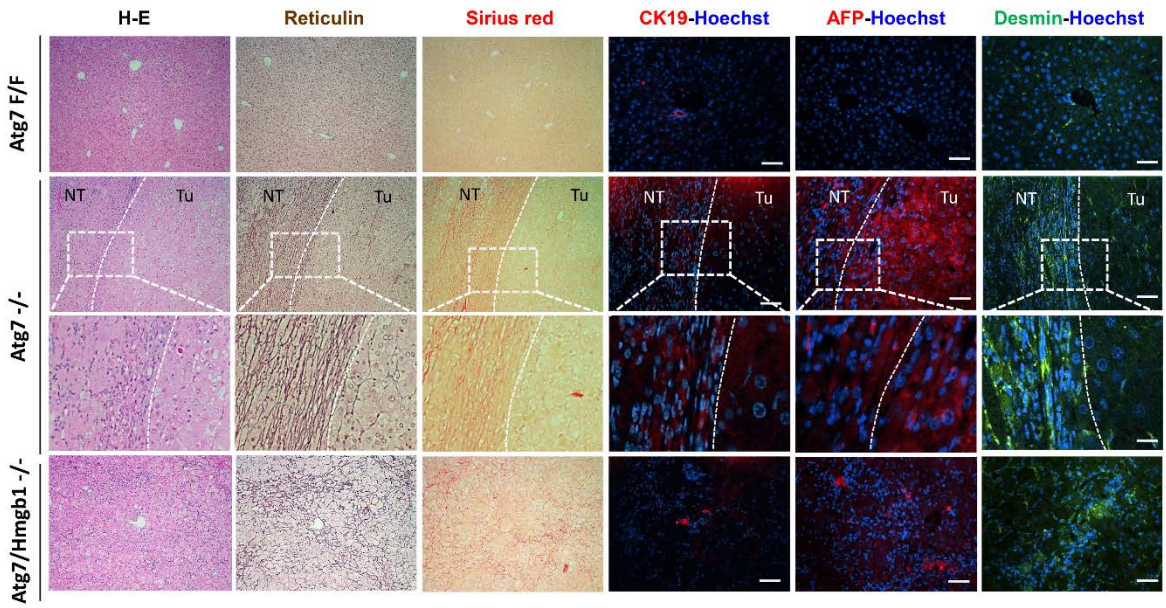

Supplemental Figure 10. Histology of tumors in Atg7-deficient livers and the impact of co-deletion of HMGB1. Representative serial sections of mice with different genotypes from 12 months old mice were stained as indicated. Framed areas were enlarged and shown in separate panels. Dotted lines indicate the border of the tumor area (Tu) and the non-tumor area (NT). Images for histology were taken at 100x magnification. Scale bar: 50 µm.

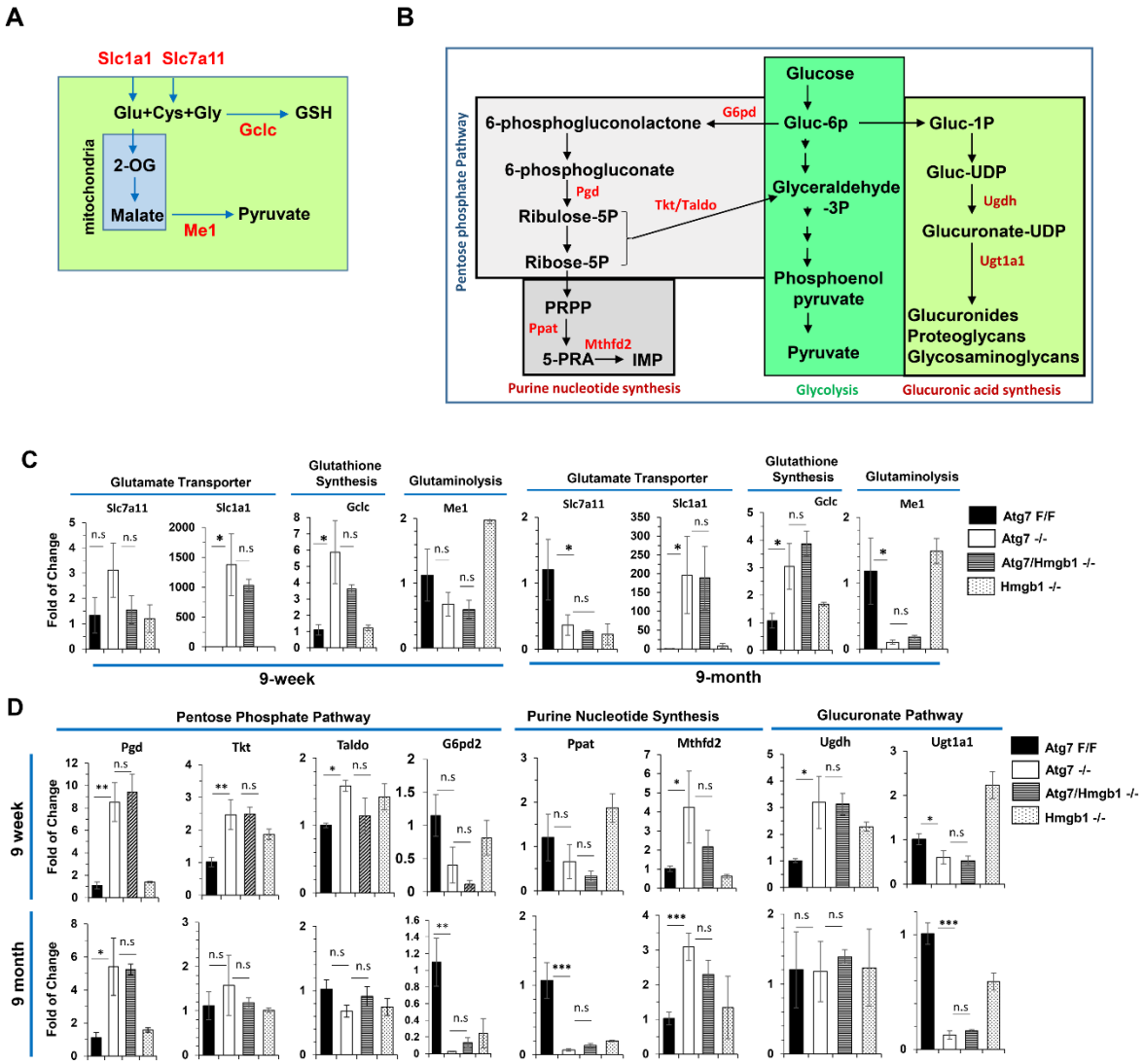

Supplemental Figure 11. Diagrams of the metabolic pathways analyzed in the study. (**A**). Glutamate is taken into the cells via the transporter, Slc1a1, whereas cysteine is taken via its transporter, Slc7a11. Glutamate, cysteine and glycine form glutathione (GSH), in which Gclc constitutes the key enzyme for the reaction. Glutamate can be converted to 2-OG and malate in the mitochondria, and eventually pyruvate in the cytosol via the key enzyme Mel. (**B**). The glucolysis pathway is intimately connected with the pentose phosphate pathway, the purine nucleotide synthesis, and glucuronic acid synthesis via multiple intermediates. The key enzymes involved in the intermediate metabolism are indicated in red. (**C-D**) Hepatic mRNA levels of genes involved in the indicated metabolic pathways were quantified (n = 3 mice/group). Data

shown are mean ± SEM. *: $p<0.05$; **: $p<0.01$; ***: $p<0.001$; n.s.: no significance, by one-way ANOVA with Duncan's post-hoc analysis.

Slc1a1: Solute carrier family 1 member 1; **Slc7a11**: Solute carrier family 7 member 11; **Gclc**: Glutamate-cysteine ligase catalytic subunit; **Me1**: Malic enzyme 1; **G6pd**: Glucose-6-phosphate dehydrogenase; **Pgd**: Phosphogluconate dehydrogenase; **Tkt**: Transketolase; **Taldo**: Transaldolase; **Ppat**: Phosphoribosyl pyrophosphate amidotransferase; **Mthfd2**: Methylenetetrahydrofolate dehydrogenase (NADP+ dependent) 2, methenyltetrahydrofolate cyclohydrolase; **Ugdh**: UDP-glucose dehydrogenase; **Ugt1a1**: UDP-glucuronosyltransferase 1a1.

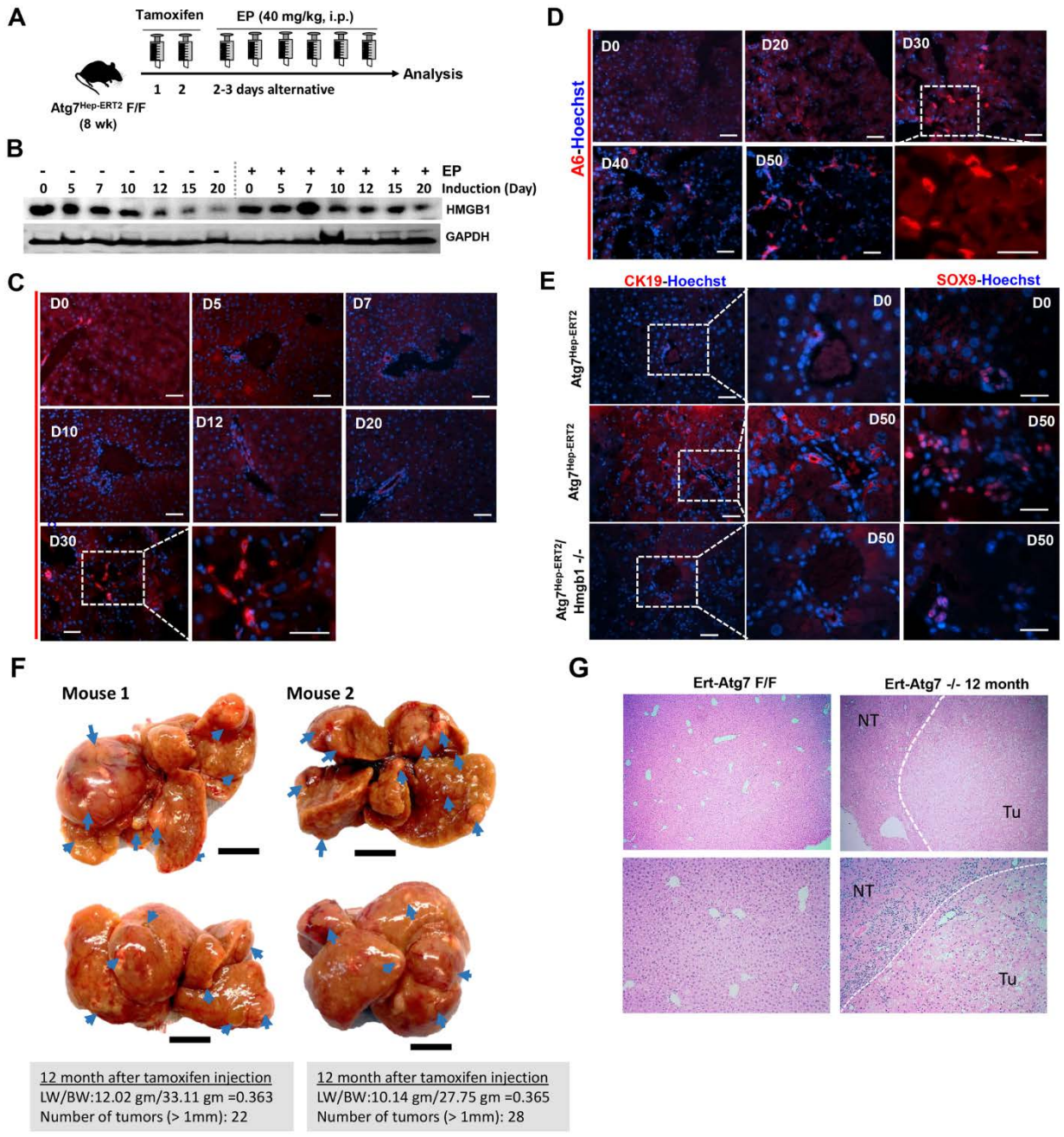

Supplemental Figure 12. HMGB1 release can be blocked by ethyl pyruvate in *Atg7*$^{Hep\text{-}ERT2}$ mice. (**A**) Scheme of *Atg7* deletion by tamoxifen and the treatment with ethyl pyruvate (EP). (**B**) Immunoblotting analysis for HMGB1 in liver lysates prepared from EP-treated or control *Atg7*$^{Hep\text{-}ERT2}$ mice that had been induced for Atg7 deletion for different times. Day 0 represents non-induced control group. (**C-D**) Liver sections from *Atg7*$^{Hep\text{-}ERT2}$ mice at different times after induction were stained for CK19 (C), or A6 (D). Quantification of CK19^{+} or A6^{+} cells is shown

in Figure 6, G-H. (**E**) Liver sections from the indicated mice at D0 and D50 after tamoxifen induction were stained for CK19 or SOX9. Quantification of $CK19^{+}$ or $SOX9^{+}$ cells is shown in Figure 6I. (**F**) Two examples of $Atg7^{Hep\text{-}ERT2}$ livers from mice induced for Atg7 deletion for 12 months. Arrows indicate the grossly observed tumors. The number of the tumors and weight of the livers were indicated. (**G**) Representative H-E stained liver sections showing the microscopic tumor nodules in induced $Atg7^{Hep\text{-}ERT2}$ mice (*Ert-Arg7 -/-*) and non-induced control $Atg7^{Hep\text{-}ERT2}$ mice (*Ert-Atg7 F/F*) after 12 months. Magnification, 40x (upper images) and 100x (lower images). White dashed lines indicate the border of the microscopic tumor area (Tu) and the non-tumor area (NT). Scale bars: 1cm (C), 50 μm (E-G).

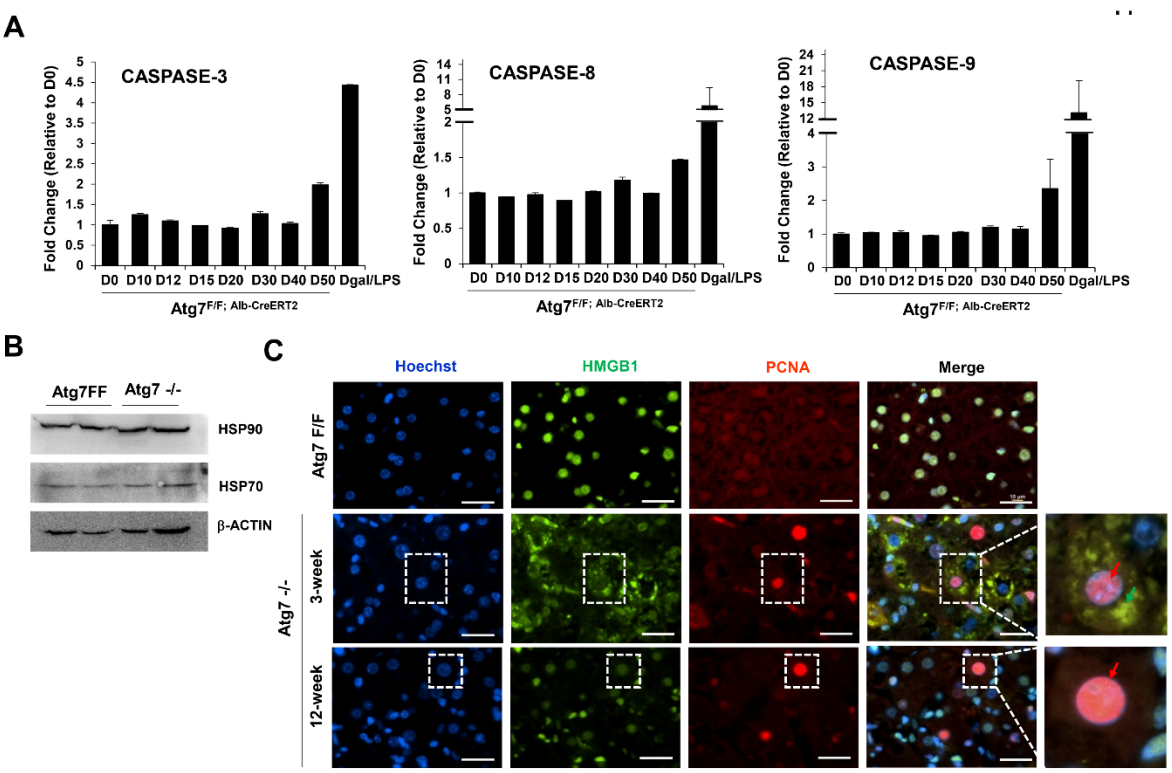

Supplemental Figure 13. Autophagy deficient livers do not present significant cellular breakdown while releasing HMGB1. (**A**) The activity of CASPAE-3, -8 and -9 was measured in liver lysates of Atg7$^{Hep\text{-}ERT2}$ mice at different days after tamoxifen treatment for different days and in the 9 weeks old Atg7-F/F mice treated with LPS/D-Gal. The LPS/D-Gal treatment served as a positive control for caspase activation. (**B**) Liver lysates were analyzed by immunoblotting assay for HSP70 and HSP90. (**C**) Immunostaining for HMGB1 and PCNA in *Atg7 F/F* and *Atg7*$^{\Delta Hep}$ liver. Boxed areas were enlarged to show the presence of PCNA signals in cells having HMGB1 in the cytosol (3-week old mouse sample), and in cells that lost HMGB1 completely (12-week old mouse sample). Data shown are mean ± SEM. n=3 mice/group. Scale bars: 10 µm.

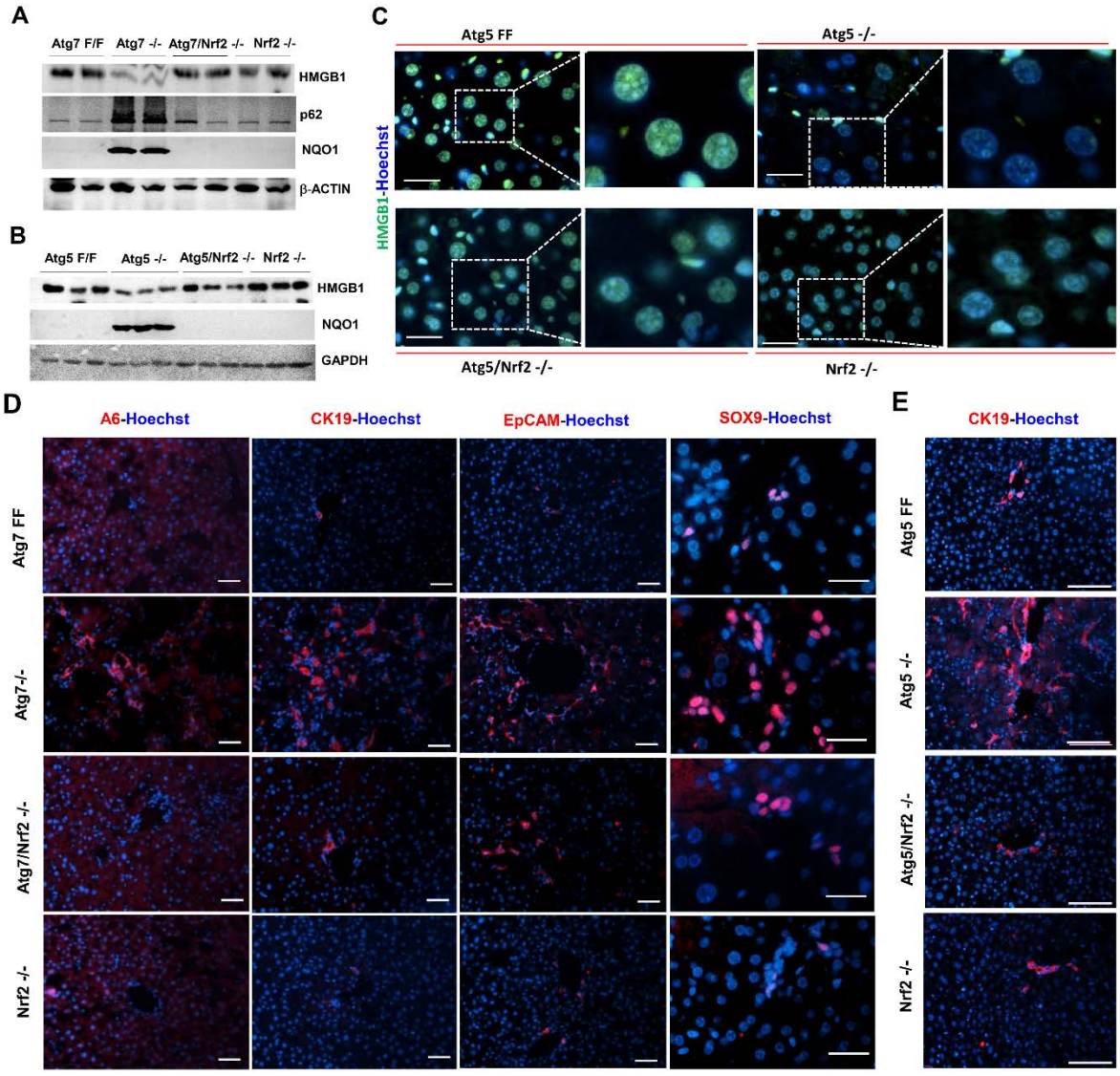

Supplemental Figure 14. **Co-deletion of *Nrf2* in *autophagy deficient* livers prevents the loss of nuclear HMGB1 and the expansion of ductular cells.** Liver samples from mice with the indicated genotypes at 9 weeks old were subjected to immunoblotting (**A-B**), or immunostaining for HMGB1 (**C**), A6, CK19, EpCAM or SOX9 (**D-E**). In A and B, each lane represented one sample. In C, the framed areas were enlarged in separate panels. Arrows indicate hepatocyte nuclei in which HMGB1 was not detected. Quantification of $CK19^+$ or $SOX9^+$ cells in D is shown in Figure 7B. Scale bars: 10 μm (HMGB1 staining in panel C, SOX9 staining in panel D); 50 μm (A6, CK19 and EpCAM staining in panel D, CK-19 staining in panel E).

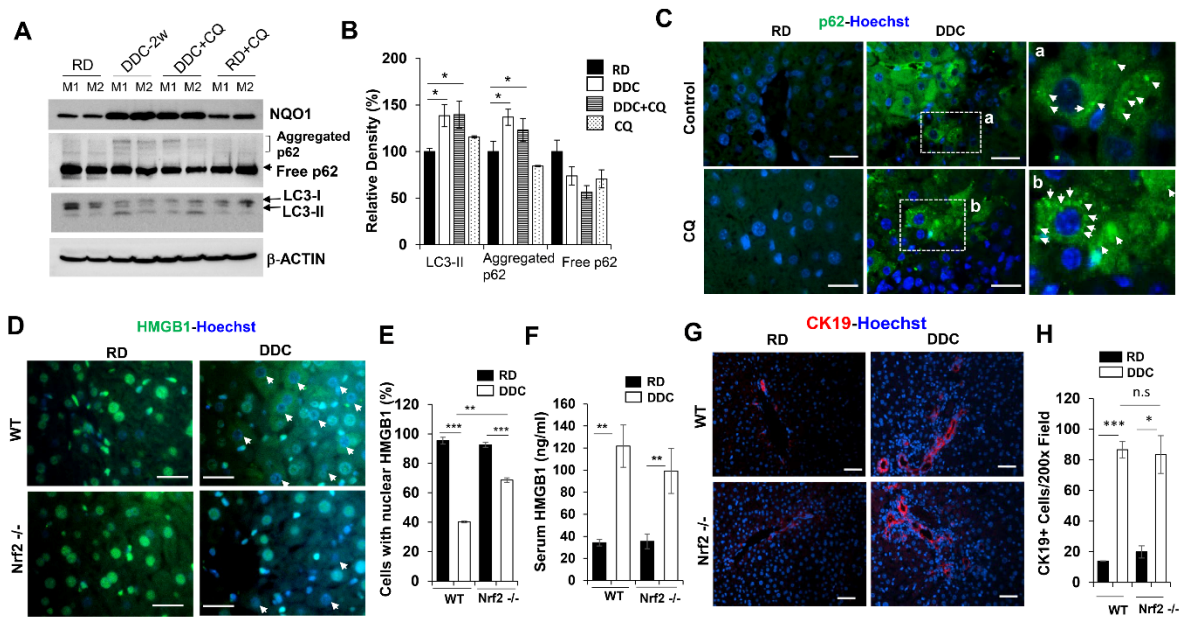

Supplemental Figure 15. Effect of Nrf2 in DDC diet-induced HMGB1 release and DR. (**A**) Liver lysates from wide type mice given regular diet (RD) or DDC diet for 2 weeks and chloroquine (CQ, 60 mg/kg, i.p.) 16 hours before analysis were analyzed by immunoblotting assay. (**B**) Densitometry analysis was conducted for LC3II and p62, which were normalized to β-actin and the control RD group. (**C**) Immunostaining for p62 in mice treated as in A. Enlarged areas (a-b) were displayed in separate panels. Arrows indicate aggregated p62 puncta. (**D-E**) Livers from mice with the indicated genotypes and the given diet for 2 weeks were stained for HMGB1 (D). Arrows indicate nuclei in which HMGB1 was not detected, which was quantified (E, n=3 mice/group). Wild type values were obtained from Supplemental Figure 6C. (**F**) Serum HMGB1 was measured for mice treated as in D (n=3-9 mice/group). Wild type values were obtained from Supplemental Figure 6D. (**G-H**) Livers from mice treated as in D were immunostained for CK19 (G) and the number of $CK19^{+}$ cells was quantified (H, n=3 mice/group). Data shown are mean ± SEM. *: p<0.05; **: p,0.01, ***: p<0.001; n.s.: no significance, by one way ANOVA with Duncan's methods post-hoc analysis. Scale bars: 10 μm (C-D), 50 μm (G).

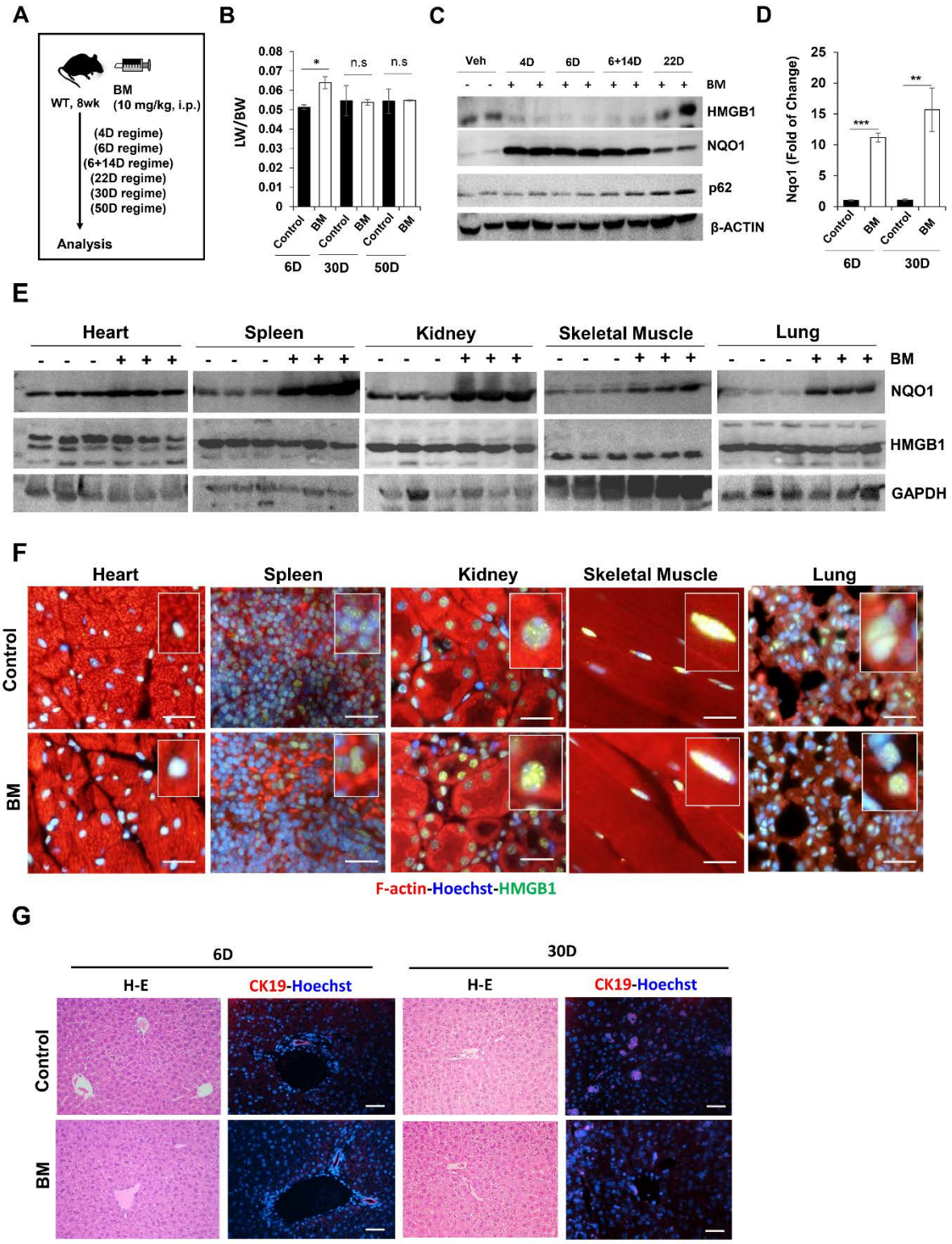
A
WT, 8wk
BM
(10 mg/kg, i.p.)
(4D regime)
(6D regime)
(6+14D regime)
(22D regime)
(30D regime)
(50D regime)
Analysis
B
LW/BW
0.08
0.07
0.06
0.05
0.04
0.03
0.02
0.01
0
*
n.s
n.s
Control
BM
6D
30D
50D
C
Veh
4D
6D
6+14D
22D
BM
HMGB1
NQO1
p62
β-ACTIN
D
Nqo1 (Fold of Change)
25
20
15
10
5
0
***
**
6D
30D
E
Heart
Spleen
Kidney
Skeletal Muscle
Lung
BM
NQO1
HMGB1
GAPDH
F
Heart
Spleen
Kidney
Skeletal Muscle
Lung
Control
BM
F-actin-Hoechst-HMGB1
G
6D
30D
H-E
CK19-Hoechst
H-E
CK19-Hoechst
Control
BM

Supplemental Figure 16. Activation of Nrf2 by bardoxolone methyl. (A) Scheme of bardoxolone methyl (BM) treatment in wild type (WT) mice. BM was intraperitoneally administered at 10 mg/kg in 6 different regimes. In the 4D or 6D regime: BM was given daily for 4 days or 6 days and samples were collected on day 5 or day 7, respectively. In the 6+15D regime, BM was given daily for 6 days followed by a maintenance schedule of once every 3 days for 5 times. Liver samples were collected the next day after the last treatment. In the 22D sample group, BM was given every day for 6 days and sample were collected on day 22. In the 30D regime, BM was given daily for 30 days and samples were collected on day 31. In the 50D regime, BM was given twice a week for 7 weeks, and samples were collected on day 50. (**B**) WT mice were given vehicle control or BM in a 6D, 30D or 50D regime. Liver weight/Body weight ratios were measured (n= 3-6 mice/group). (**C**) Immunoblotting analysis of liver lysates from WT mice receiving the indicated BM treatment regimes. Each lane represents one sample. (**D**) Hepatic mRNA levels of Nqo1 in mice receiving 6D or 30D (n=3-5 mice/group). (**E**) Immunoblotting analysis of tissue lysates prepared from WT mice receiving the 6D regime. (**F**) Immunostaining for HMGB1 on tissue sections from WT control mice or mice receiving BM in the 6D regime. Insets demonstrate enlarged cells with the HMGB1 nuclear staining. (**G**) Liver sections from mice receiving a 6D or 30D BM treatment regime were H-E-stained (200x) or immunostained for CK19. Data shown are mean ± SEM. *: $p<0.05$, **: p,0.01, ***: $p<0.001$; n.s.: no significance, by *Student's* t-test. Scale bar: 10 µm (F), 50 µm (G).

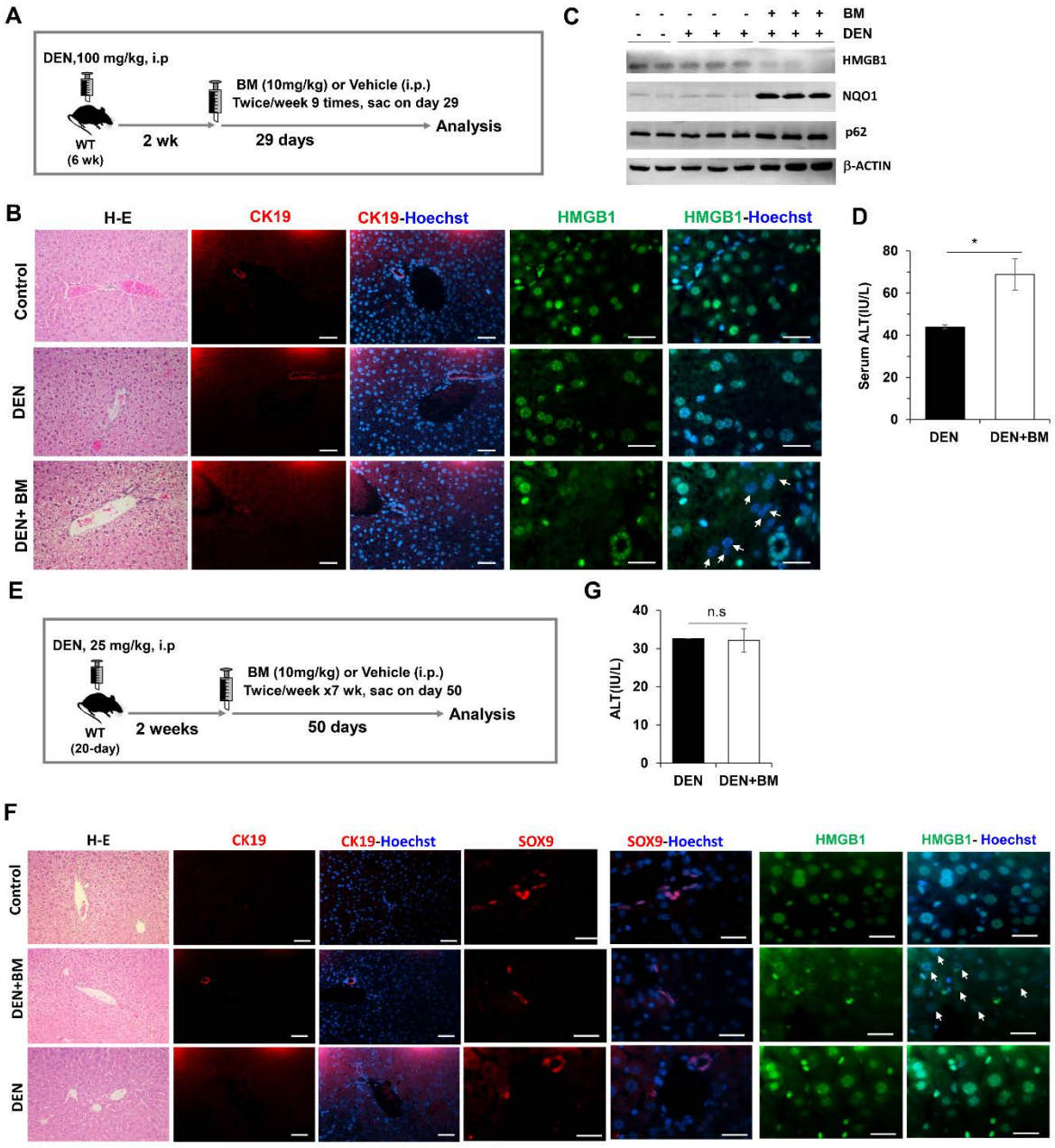

Supplemental Figure 17. Combined treatment of BM with DEN did not cause ductular reaction. (**A**) Diagram of the treatment with DEN and BM in adult mice. (**B**) The liver sections of mice given in the indicated treatment were subjected to H-E staining (200x), HMGB1 staining, or CK19 staining. (**C**) Liver lysates of adult mice given the indicated treatments were analyzed by immunoblotting assay. (**D**) Serum level of ALT in adult mice treated with DEN or DEN plus BM (n=4-5 mice/group). (**E**) Diagram of the treatment with DEN and BM in neonatal mice. (**F**) The liver sections of mice given in the indicated treatment were subjected to H-E

staining (200x), HMGB1 staining, or CK19 staining, or SOX9 staining. (**G**). Serum level of ALT in neonatal mice treated with DEN (n=4 mice/group) or DEN plus BM (n=6 mice/group). Data shown are mean ± SEM. *: $p<0.05$; n.s.: no significance, *Student's* t-test. Scale bar: 50 μm (CK19 in B and F), 10 μm (HMGB1 in B and F, SOX9 in F). Arrows in panels B and F indicate hepatocyte nuclei without HMGB1.

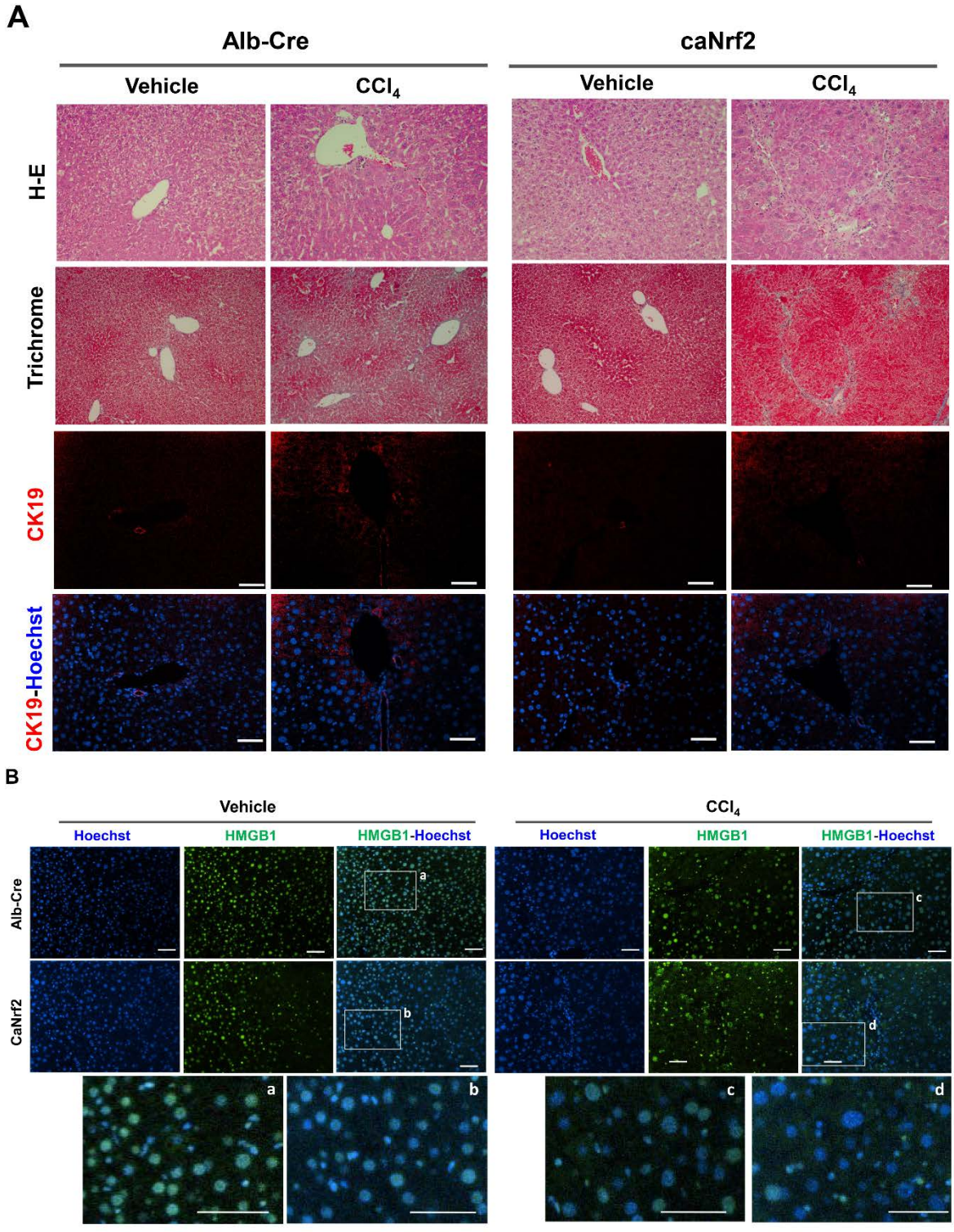

Supplemental Figure 18. NRF2 activation in combination of CCl_4 treatment causes HMGB1 release but not ductular reaction. *caNrf2* transgenic mice or control *Alb-Cre* mice were given CCl_4 (0.2 mg/g body weight) or vehicle control (olive oil) every three days for 45

days. Liver sections were examined by H-E staining or Trichrome staining (**A**, 200x), or by immunostaining for CK19 (**A**), or HMGB1 (**B**). Boxed areas (a-d) in panel B were enlarged in separate panels. While fibrosis was noticeable, there was no obvious ductular reaction following CCl_4 treatment in either control Alb-Cre mice or the caNrf2 mice. CCl_4 or *caNrf2* alone can both cause HMGB1 release (b, c). The combination of the two caused a more complete loss of HMGB1 (d). Scale bar: 50 μm.

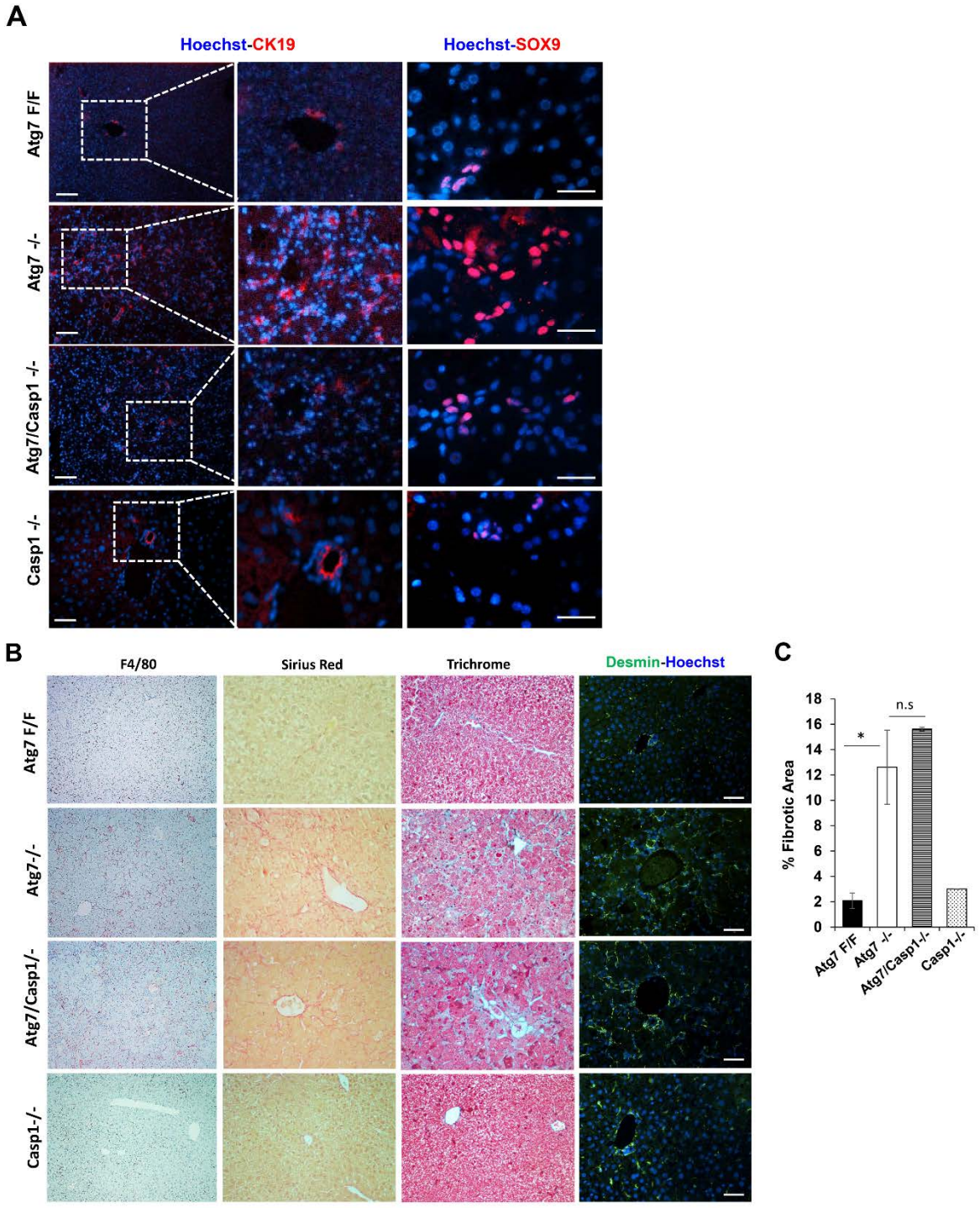

Supplemental Figure 19. *Caspase-1* co-deletion in *Atg7$^{\Delta Hep}$* liver does not protect against hepatomegaly, liver injury, liver inflammation and fibrosis. (**A-B**) Liver sections of 9-week old mice of different genotypes were stained as indicated. Quantification of CK19^{+} or SOX9^{+} cells is shown in Figure 8H. (**C**). Percentage of fibrotic areas based on trichrome staining were

defined using ImageJ software (n=3 mice/group**)**. Histology images were taken at 200x. Data shown are mean ± SEM. *: $p<0.05$; n.s.: no significance; by one-way ANOVA with Duncan's post-hoc analysis. Scale bar: 10 μm (SOX9 staining in panel A, Desmin staining in panel B,); 50 μm (CK19 in panel A).

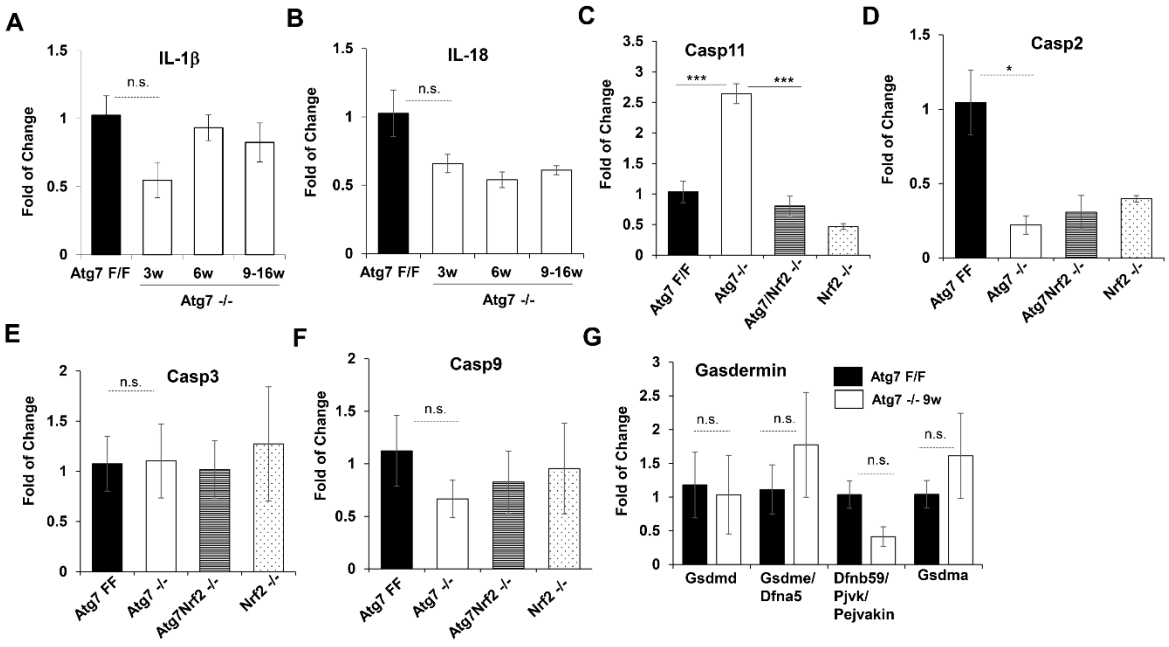

Supplemental Figure 20. Increased expression of *Caspase-11* in autophagy deficient livers. (**A-B**) The hepatic mRNA levels of IL-1β and IL-18 in the Atg7F/F mice and Atg7$^{\Delta Hep}$ (*Atg7-/-*) mice at different ages were quantified by RT-PCR. (**C-F**) The hepatic mRNA levels of *Casp11*, *Casp2*, *Casp3* and *Casp9* in mice of the indicated genotypes were quantified by RT-PCR. Primer Set 4 located in Exon 9 was used for *Casp11* amplification in panel C. (**G**) The hepatic mRNA levels of four GASDERMIN family members in the Atg7F/F mice and Atg7$^{\Delta Hep}$ (*Atg7-/-*) mice at different ages (week) were quantified by RT-PCR. Data shown are mean ± SEM. n=3 mice per group for all panels. *: $p<0.05$, ***: $p<0.001$, n.s.: no significance, by two-side *Student's* t test.

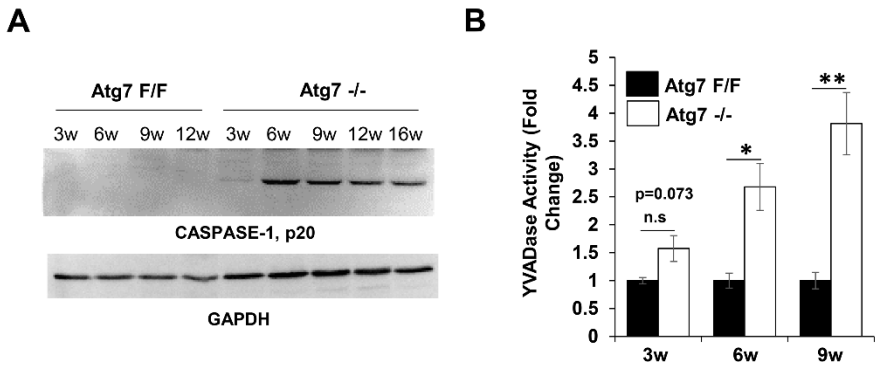

Supplemental Figure 21. Activation of CASPASE-1 in *Atg7$^{\Delta Hep}$* mice at different ages. (**A**) Immunoblotting analysis for activated CASPASE-1 p20 subunit in *Atg7 F/F* and *Atg7$^{\Delta Hep}$* (Atg7 -/-) livers at different ages (316 weeks). (**B**) Total liver lysate prepared from *Atg7 F/F and Atg7$^{\Delta Hep}$* (*Atg7* -/-) liver mice were analyzed at different ages (3, 6, and 9 weeks) for YVADase (CASPASE-1) activity (n= 3 mice /group). Data shown are mean ± SEM. *: $p<0.05$, **: $p<0.01$, n.s.: no significance, by two-side Student's t-test.

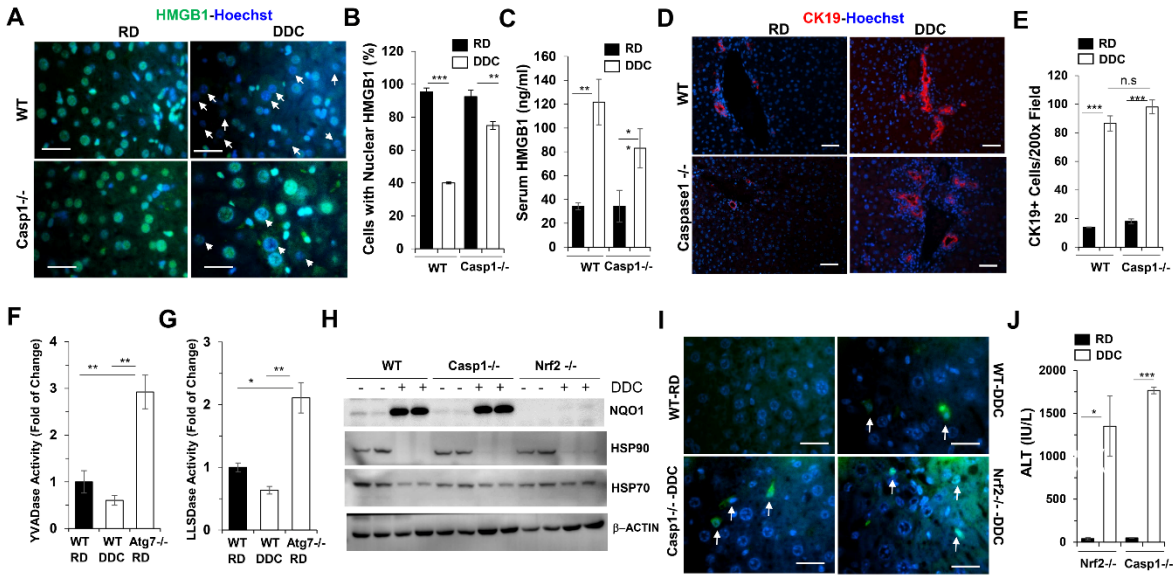

Supplemental Figure 22. The role of CASPASE-1 in DDC diet-induced HMGB1 release and DR. (**A-B**). Liver sections of wild type (WT) and *Caspase-1* deficient mice given regular diet (RD) or DDC diet for 2 weeks were stained for HMGB1 (A). Arrows indicate hepatocyte nuclei in which HMGB1 was not detected, which was quantified (B). The values of WT mice were obtained from Supplemental Figure 6C. (**C**). Serum HMGB1 was measured from mice as treated in A. The values of WT mice were obtained from Supplemental Figure 6D. (**D-E**). Liver sections of mice as in panel A were immunostained for CK-19 (D). The number of $CK19^{+}$ cells was quantified (E). (**F-G**). YVADase (F) and LLSDase (G) activities were measured in the liver lysates from wild type mice given RD or DDC for 2 weeks. Liver lysates from *Atg7*-deficinet mice fed with RD were used as positive controls. (**H**). Immunoblotting analysis of liver of WT, *Casp1-/-* and *Nrf2-/-* mice given RD or DDC for 2 weeks. (**I**). TUNEL analysis of the livers of WT, *Casp1*- or *Nrf2*-deficient mice given RD or DDC for 2 weeks. (**J**). ALT levels of mice with indicated genotypes that were given RD or DDC for 2 weeks. Data shown are mean ± SEM. n= 3 mice/group. *: p<0.05; **: p<0.01; ***: p<0.001; n.s.: no significance, by two-side *Student's* t-test. Scale bar: 10 μm (A), 50 μm (D, I).

Supporting Table 1. Antibodies used in immunoassays

Antibody/Species	Source/Catalogue Number/Dilution
Atg7/Rabbit	Cell Signal/2631/1:1000
A6/Rat	Gift from Dr.Valentina Factor(NCI, Washington D.C.)/1:100
Alexa-488-antiRabbit	InVitrogen/A-11034/1:500
alpha feto protein(AFP)/Goat	Santa Cruz(C-19)/sc-8108/1:200
Caspase 11/Rat	Cell Signal/14340/1:1000
Caspase-1/Rabbit	Santa Cruz/sc-514/1:500
CD3/Rat	BD Pharmagen/557306/1:100
CD45R/Rat	BD Pharmagen/553089/1:100
CK19/TROMA-III/Rat	Developmental Studies Hybridoma Bank(University of Iowa, Iowa City, IA)/1DB-001-0000868971/1:200
Cy3-Anti Rat	Jackson ImmunoResearch Laboratories Inc/712-165-150/1:500
Desmin/Rabbit	Thermo /RB9014P0/1:200
EpCAM/Rat	eBioscience/Ref:14-5791-82/1:100
Erk/Rabbit	Cell Signaling/9102/1:1000
F4/80/Rat	Bio-Rad/MCA497G/1:100
Gapdh/Mouse	Novus/NB300-21/1:3000
GasderminD/Mouse	Santa Cruz/sc-393656/1:200
Gli2/Rabbit	Genetex/GTX27195/1:1000
GST/Rabbit	Cell Signaling/2625/1:1000
Histone	Cell Signal/4499/1:1000
Hmgb1/Rabbit	Abcam/ab18256/1:1000
HNF4a/Goat	Santa Cruz/sc-6556/1:400
HRP-labeled Goat secondary antibody	Jackson ImmunoResearch Laboratories Inc/705-165-147/1:5000
HRP-labeled Mouse secondary antibody	Jackson ImmunoResearch Laboratories Inc/115-035-062/1:5000
HRP-labeled Rabbit secondary antibody	Jackson ImmunoResearch Laboratories Inc/111-035-045/1:5000
HSP70/Rabbit	Cell Signal/4872/1:1000
HSP90/Rabbit	Cell Signal/4874/1:1000
LC3B/Rabbit	Sigma/L7543/1:1000
Nqo1/Rabbit	Abcam/ab34173/1:3000
Nrf2/Rabbit	Santa Cruz/sc-722/1:200
p62/Mouse	Abnova/H00008878-M01/1:1000
PCNA/Mouse	Signet Pathology System Inc/P1172/1:200
p-ERK/Rabbit	Cell Signaling/4370/1:1000
RAGE/Mouse	Santa Cruz/sc-365154/1:200
Shh/Mouse	Santa Cruz/sc-365112/1:200

Sox9/Rabbit	EMB Millipore/AB5535/1:1000
Vps34/Rabbit	Abgent/AP8014a/1:500
α-Smooth Muscle antigen(αSMA)/Rabbit	Thermo/PA5-19465/1:1000
β-Actin/Mouse	Sigma/5441/1:5000

Supporting Table 2. Primers used in PCR assays

Gene name	Forward primer	Reverse Primer
Actin	5'-GACGGCCAGGTCATCACTATTG-3'	5'-AGGAAGGCTGGAAAAGAGCC-3'
AFP	5'-CTCAGCGAGGAGAAATGGTC-3'	5'-GAGTTCACAGGGCTTGCTTC-3'
Albumin	5'-GACGTGTGTTGCCGATGAGT-3'	5'-GTTTTCACGGAGGTTTGGAATG-3'
a-SMA	5'-ATCGTCCACCGCAAATGC-3'	5'-AAGGAACTGGAGGCGCTG-3'
Caspase 1	5'-ACAAGGCACGGGACCTATG-3'	5'-TCCCAGTCAGTCCTGGAAATG-3'
Caspase 11 Set 1	5'-GCCACTTGCCAGGTCTACGAG-3'	5'-AGGCCTGCACAATGATGACTTT-3'
Caspase 11 Set 4	5'-TTGGCCAAGGATCACATTCTATTC-3'	5'-TATGGAACAGAATCCCACTGTGT-3'
Caspase 2	5'-GGAGCAGGATTTTGGCAGTGT-3'	5'-GCCTGGGGTCCTCTCTTTG-3'
Caspase 3	5'-ATGGAGAACAACAAAACCTCAGT-3'	5'-TTGCTCCCATGTATGGTCTTTAC-3'
Caspase 9	5'-TCCTGGTACATCGAGACCTTG-3'	5'-AAGTCCCTTTCGCAGAAACAG-3'
Col1a1	5'-ACGGCTGCACGAGTCACAC-3'	5'-GGCAGGCGGGAGGTCTT-3'
Ctgf	5'-GGGCCTCTTCTGCGATTTC-3'	5'-ATCCAGGCAAGTGCATTGGTA-3'
Dfna5	5'-CCTGGCCTACAGAGAGTTCG-3'	5'-TCTCTAGGTGCAGGGTTGCT-3'
Dfnb59	5'-GGATCTGATTCCATCGCAGT-3'	5'-CTTGATTGGCGGATCAAACT-3'
F4/80	5’-TGCATCTAGCAATGGACAGC-3’	5’-GCCTTCTGGATCCATTTGAA-3’
G6pd2	5'-CAGAGCAGGTGACCCTAAGC-3'	5'-GCATAGCCCACAATGAAGGT-3'
Gclc	5'-GTGGACGAGTGCAGCAAG-3'	5'-GTCCAGGAAATACCCCTTCC-3'
Gli1	5'-CAGGGAAGAGAGCAGACTGAC-3'	5'-CGCTGCTGCAAGAGGACT-3'
Gsdma	5'-GGGCGAAGCTCACTACTCAC-3'	5'-GGTCACTTCGTGTCCCTTGT-3'
Gsdmd	5'-ACCAGAACCGGAGTGTTTTG-3'	5'-GCACTTCCTCCTTTGTCTGC-3'
Hhip	5'-CTACTTGGGCCAGATGGAAG-3'	5'-CTCCAAGTAAGGCTCCTTGAAC-3'
Hmgb1	5'-CGCGGAGGAAAATCAACTAA-3'	5'-GCAGACATGGTCTTCCACCT-3'
IGF2	5'-TGAGAAGCACCAACATCGAC-3'	5'-CTTCTCCTCCGATCCTCCTG-3'
IL-18	5'-ACGTGTTCCAGGACACAACA-3'	5'-ACAAACCCTCCCCACCTAAC-3'
IL-1b	5'-GCTGCTTCCAAACCTTTGAC-3'	5'-TGTCCTCATCCTGGAAGGTC-3'
Me1	5'-GCAGCTCTTCGAATAACCAAG-3'	5'-AAGTGAGCAATCCCCAAGG-3'
Mthfd2	5'-TCCAAATCTGATCACAGCTGAC-3'	5'-AACCAGCTTTCTTCTTGACTCC-3'
Nqo1	5'-AGCGTTCGGTATTACGATCC-3'	5'-AGTACAATCAGGGCTCTTCTCG-3'
Patched 1	5'-CCTCCTTTACGGTGGACAAAC-3'	5'-ATCAACTCCTCCTGCCAATG-3'
Pgd	5'-GGGCACTTTGTGAAGATGGT-3'	5'-AACAGCTCTTTGCCGTCAGT-3'
PP1A	5’-CTCAGCCTATTTAGAAACAGACT-3’	5’TCTCCTGGGCCTGCAAAAT-3’
Ppat	5'-GCATACACCCCTCCTCAAGA-3'	5'-GGGCGCTTCTTTCATTAAGTT-3'
RAGE	5'-GGGAGGCCTGGGAGTAGTAG-3'	5'-ACGTTCCTCCTCATCCTCCT-3'
Rex3	5'-TACTCCTGGGCCTATCCTTG-3'	5'-GCAGCAGGAGGAGGAAGAG-3'

Slc1a1	5'-TGCTGAAGCTGGTCATTTTG-3'	5'-CTGAGTGACACCAGGCTTGA-3'
Slc7a11	5'-TTTACTCGGACCCATTCAGC-3'	5'-CGTCTGAACCACTTGGGTTT-3'
Smo	5'-GCAAGCTCGTGCTCTGGT-3'	5'-GGGCATGTAGACAGCACACA-3'
Taldo	5'-GACGCTCATCTCTCCCTTTG-3'	5'-GGGAGATGGTGAGGAAGTCA-3'
Tkt	5'-GCCAGGTTCAGAGCAAAAAG-3'	5'-CTCGGCAATGTAGCACTCAA-3'
Ugdh	5'-CTGAATCTGCCCGAAGTAGC-3'	5'-GCAAACCTCCTCCTCTGGTA-3'
Ugt1a1	5'-AAACTGTCATCAACAACAAGAGCTA-3'	5'-GCCAGGTCCAGAGGCTCTAT-3'